Strong pinning in the hole-doped pnictide superconductor $La_{0.34}Na_{0.66}Fe_2As_2$ 🔵EP

Shyam Sundar 🔵, S. Salem-Sugui, A. D. Alvarenga, M. M. Doria, Yanhong Gu, Shiliang Li, Huiqian Luo, and L. Ghivelder

COLLECTIONS

EP   This paper was selected as an Editor's Pick

🌐 **View Online**   ⬆ **Export Citation**   🔴 **CrossMark**

ARTICLES YOU MAY BE INTERESTED IN

First-principles assessment of thermoelectric properties of $CuFeS_2$
Journal of Applied Physics **125**, 125102 (2019); https://doi.org/10.1063/1.5088165

Alignment and small oscillation of superparamagnetic iron oxide nanoparticle in liquid under alternating magnetic field
Journal of Applied Physics **125**, 123901 (2019); https://doi.org/10.1063/1.5079899

Temporal evolution of photoinduced optical chirality in nanostructured light-sensitive waveguide thin films: Simultaneous excitation of TE_0 and TE_1 modes
Journal of Applied Physics **125**, 123101 (2019); https://doi.org/10.1063/1.5079506

Strong pinning in the hole-doped pnictide superconductor La$_{0.34}$Na$_{0.66}$Fe$_2$As$_2$ ⓔⓅ

Shyam Sundar,[1,a),b)] ⓘ S. Salem-Sugui, Jr.,[1] A. D. Alvarenga,[2] M. M. Doria,[1] Yanhong Gu,[3,4] Shiliang Li,[3,4,5] Huiqian Luo,[3,5] and L. Ghivelder[1]

AFFILIATIONS

[1]Instituto de Fisica, Universidade Federal do Rio de Janeiro, 21941-972 Rio de Janeiro, RJ, Brazil
[2]Instituto Nacional de Metrologia Qualidade e Tecnologia, 25250-020 Duque de Caxias, RJ, Brazil
[3]Beijing National Laboratory for Condensed Matter Physics, Institute of Physics, Chinese Academy of Sciences, Beijing 100190, China
[4]School of Physical Sciences, University of Chinese Academy of Sciences, Beijing 100049, China
[5]Songshan Lake Materials Laboratory, Dongguan, Guangdong 523808, China

[a)]**Present address:** Department of Physics, Simon Fraser University, Burnaby, British Columbia V5A 1S6, Canada.
[b)]shyam.phy@gmail.com

ABSTRACT

We present magnetization studies as a function of time, temperature, and magnetic field for $H \parallel$ c-axis, in a hole-doped pnictide superconductor, La$_{0.34}$Na$_{0.66}$Fe$_2$As$_2$, with $T_c \approx 27$ K. The obtained vortex phase-diagram shows that the magnetic irreversibility line is very close to the mean-field superconducting transition line, similar to the low T_c superconductors, evidencing a strong pinning behavior. The irreversibility line does not follow a power law behavior with (T_c-T); however, it is well described using an expression developed in the literature, considering the effect of disorder in the system. The critical current density estimated using the Bean critical-state model is found to be of the order of 10^5 A/cm^2 below 12 K in the limit of zero magnetic field. A plot of the normalized pinning force density as a function of the reduced magnetic field at different temperatures shows good scaling, and the analysis suggests that the vortex pinning is due to normal point-like pinning centers. The temperature dependence of the critical current density suggests that the pinning due to the variation in the charge carrier mean free path alone is not sufficient to explain the experimental data. The magnetic relaxation rate as a function of temperature and magnetic field is also studied.

I. INTRODUCTION

Superconductivity in Fe-pnictides is a field of great interest for fundamental science as well as for technological advancement.[1–4] Since the advent of iron-based superconductors (IBS), many new superconductors have been discovered in different families of this interesting class of high T_c superconducting compounds.[3] Among the different families of IBS, the 122-class is more interesting in terms of technological purposes and also due to the availability of good quality sizable single crystals.[3–8] Recently, a new platform in the 122-pnictide family was discovered with a chemical formula (La$_{0.5-x}$Na$_{0.5+x}$)Fe$_2$As$_2$ [(La,Na)-122 family].[9,10] It is an interesting and unique member of the 122-family, which allows the investigation of the electron-hole asymmetry, because in this system, the doping occurs at the La-Na site with no change taking place in the Fe-As layers, as opposed to the doping in other 122-pnictide systems.[9–11]

Vortex dynamics and pinning mechanism in IBS is quite interesting due to its salient features[12–15] such as low Ginzburg number (G_i),[16] small anisotropy,[17] high intergrain connectivity,[18] high upper critical field,[19] and moderate T_c.[20] These properties are vital for technological applications of type-II superconductors.[3,4] In spite of low Ginzburg number (G_i), the vortex phase-diagram of IBS and low-T_c superconductors (LTS) are quite different in the sense that the upper critical-field, $H_{c2}(T)$, and the irreversibility line, $H_{irr}(T)$, are separated by a broad vortex-liquid region in IBS,[21] whereas in LTS, no appreciable vortex-liquid region exists.

Our motivation in the present study is to explore the vortex dynamics in this recently discovered 122-type of IBS.[11]

In this work, we report a study of vortex dynamics in a single crystal of the hole-doped $La_{0.34}Na_{0.66}Fe_2As_2$ superconductor using the isofield temperature dependence of the magnetization, $M(T)$, the isothermal magnetic field dependence of the magnetization, $M(H)$, and magnetic relaxation, $M(t)$, measurements for $H \parallel$ c-axis. The obtained vortex phase-diagram shows that the irreversibility line, H_{irr}, is very close to the mean field $T_c(H)$-line, similar to the behavior in LTS. Critical current density, J_c, and the pinning mechanism are analysed using the models developed by Griessen *et al.*[22] and Dew-Hughes,[23] respectively. The magnetic relaxation rate as a function of temperature and magnetic field is discussed.

II. EXPERIMENTAL

The hole doped $La_{0.34}Na_{0.66}Fe_2As_2$ crystal was obtained accidentally when growing the LaFeAsO single crystal with NaAs and NaF flux. Details of the crystal growth are given in Ref. 11. The obtained $La_{0.34}Na_{0.66}Fe_2As_2$ crystals were characterized using different experimental techniques (see Ref. 11), which confirm the good quality of the crystals. These crystals have the same structure as $A_eFe_2As_2$ (A_e = alkaline earth metal, e.g., Ca, Sr, Ba) with La and Na occupying the A_e site. A sample from the same batch as in Ref. 11 with mass $m = 0.1348$ mg and dimensions 1.54 mm $\times$ 1.52 mm $\times$ 0.016 ($\pm$ 0.002) mm was used in the present study. The magnetic measurements were made using a Quantum Design vibrating sample magnetometer (VSM) built in a 9 T physical property measurement system (PPMS), with magnetic fields applied parallel to the c-axis of the sample. $M(T)$ measurement at $H = 10$ Oe shows a superconducting transition $T_c \approx 27$ K and a transition width $\Delta T_c \approx 4$ K. All magnetic measurements were obtained after a standard zero field cooled (ZFC) procedure. Isothermal $M(H)$ curves were measured with a ramp field $dH/dt = 50$ Oe/s and obtained in five quadrants. Isofield $M(T)$ curves were continuously measured during a slow heating [and cooling in the case of field cooled (FC) curves] of $dT/dt = 0.3$ K/s. $M(t)$ curves were obtained for a span of time 1.5 h at various temperatures with $H = 30$ kOe and at various magnetic fields at $T = 16$ K.

III. RESULTS AND DISCUSSION

Figure 1(a) shows selected isofield $M(T)$ curves obtained in both ZFC and FC modes. The ZFC and FC curves separate just below the temperature region where the magnetization appears to be flat, with a subtle diamagnetic inclination (normal background). Figure 1(b) shows a detail of the $M(T)$ curve obtained for $H = 1$ T, where the background selected in the normal region follows the expression $M_{back} = a(H) - b(H)T$, where $a(H)$ and $b(H) > 0$ are constants for each magnetic field. For curves with $H > 3$ kOe, $a(H)$ is negative, which is due to the contribution from a sample holder. This background contribution was observed for all $M(T)$ curves and subtracted in the following analysis. The inset of Fig. 1(b) shows a detail of the main plot near the transition which clearly shows that it is difficult to resolve the difference between $T_c(H)$, the mean field transition temperature defined as the temperature for which magnetization becomes diamagnetic with decreasing temperature, and T_{irr}, which marks the irreversible temperature at which
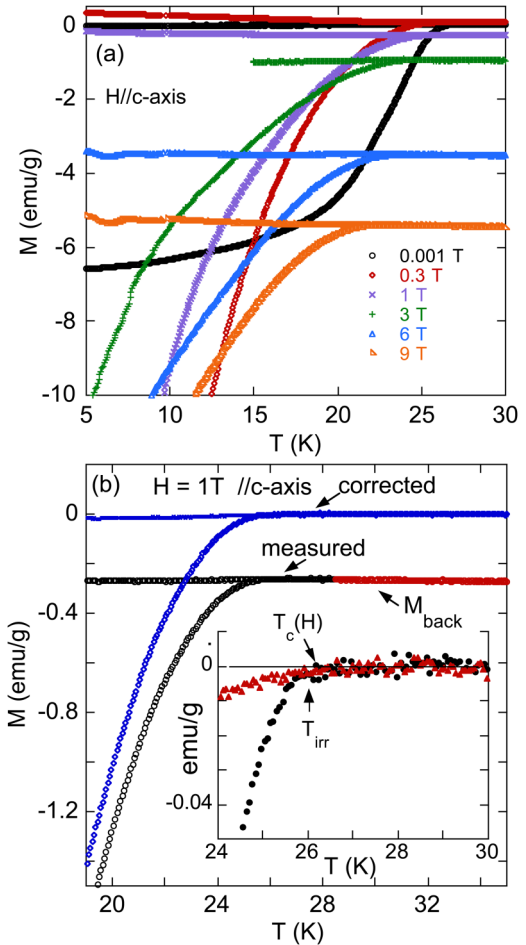

FIG. 1. (a) Selected isofield $M(T)$ curves as measured. (b) Isofield $M(T)$ curves with and without background subtraction for $H = 1$ T. The inset shows an enlarged plot at temperatures near $T_c(H)$.

the ZFC and FC curves separate. This behavior has been observed for all $M(T)$ curves.

Therefore, we decided to obtain the irreversible field, H_{irr}, from isothermal hysteresis $M(H)$ curves as shown in Fig. 2(a), which was limited to our maximum magnetic field of 9 T. It is possible to see from Fig. 2(a) that all $M(H)$ curves show a small asymmetry due to a rotation of the x-axis, which is an effect due to the sample holder signal. This rotation can be fixed by calculating the equilibrium magnetization, $M_{eq} = (M^+ + M^-)/2$, where M^+ is the increasing field branch of a $M(H)$ and M^- is the decreasing field branch. The new increasing and decreasing fields branches can then be obtained after subtracting the measured $M(H)$ from M_{eq}, which produces symmetric $M(H)$ curves with respect to the x-axis, evidencing that bulk pinning dominates in the sample. We define H_{irr} as the magnetic field where the field increasing and field decreasing branches of the $M(H)$ curves merge together within the equipment resolution, $\sim 1 \times 10^{-5}$ emu. The critical current density

associated with each $M(H)$ curve is obtained through the Bean model[24] using the expression,[25] $J_c = 20\Delta M/a(1 - a/3b)$, where $b > a$ (cm) are the single crystal dimensions defining the area perpendicular to the magnetic field, ΔM(emu/cm^3), corresponds to the width of the hysteresis curves and the resulting J_c is given in A/cm^2 units. Figure 2(b) shows the resulting $J_c(H)$ curves as obtained. The curves for $T < 12$ K show $J_c(0)$ values, the critical current at zero field, above 10^5 A/cm^2, which is considered the required threshold value for applications.[4] However, J_c suppresses relatively as fast as the magnetic field increases and shows J_c of the order of $\sim 10^4$ A/cm^2 up to 9 T (maximum field of measurements) for $T < 12$ K. We believe that the observed critical current density may be improved by introducing artificial defects as observed in other iron-pnictide superconductors.[26] Among the different families of pnictide superconductors, the 122-class is the most relevant for high field application purposes.[4] For comparison, in the case of K-doped ($x = 0.3$) 122-pnictide superconductors, the observed J_c is over 10^5 A/cm^2 in a wide temperature and magnetic field range (up to $0.8T_c$, 6 T),[27,28] whereas in the case of Co-doped ($x = 0.057$) and P-doped ($x = 0.3$) 122-pnictide superconductors, $J_c > 10^5$ A/cm^2 is observed for $T = 0.5$ T_c and $H = 6$ T.[28] Similarly, near optimal

doped Ni-122 pnictide superconductors show $J_c > 10^5$ A/cm^2 in a wide temperature and magnetic field range.[29] The effect of particle irradiation on the vortex dynamics and J_c would be interesting to explore in the present sample. A detailed review of the critical current density and pinning in bulk, thin films, tapes, and wires of IBS for technological importance is provided in Refs. 3 and 4.

The inset of Fig. 2(b) shows a selected $J_c(H)$ curve at 16 K, evidencing a change in the curvature as $J_c(H)$ approaches zero which was observed in all curves at higher temperatures. The same effect can be observed in the respective $M(H)$ curves. This change in curvature (downward to upward curvature as field increases) is usually a precursor of the peak effect occurring in $J_c(H)$ curves,[30] which is absent in our sample. The interesting point of this effect is that $J_c(H)$ approaches zero with a downward curvature, while usually it approaches zero exponentially (upward curvature).

In order to better understand this effect, we have obtained magnetic relaxation measurements, $M(t)$, as a function of magnetic field and temperature. The resulting $M(t)$ curves plotted as $\ln(M)$ vs. $\ln t$ produced the usual linear behavior, allowing us to obtain the relaxation rate $R = -d[\ln(M)]/d[\ln t]$, as shown in Fig. 3(a). Figure 3(b) shows a plot of R vs. H at $T = 16$ K, where R decreases monotonically as the field increases, evidencing the strength of the pinning as the field increases.
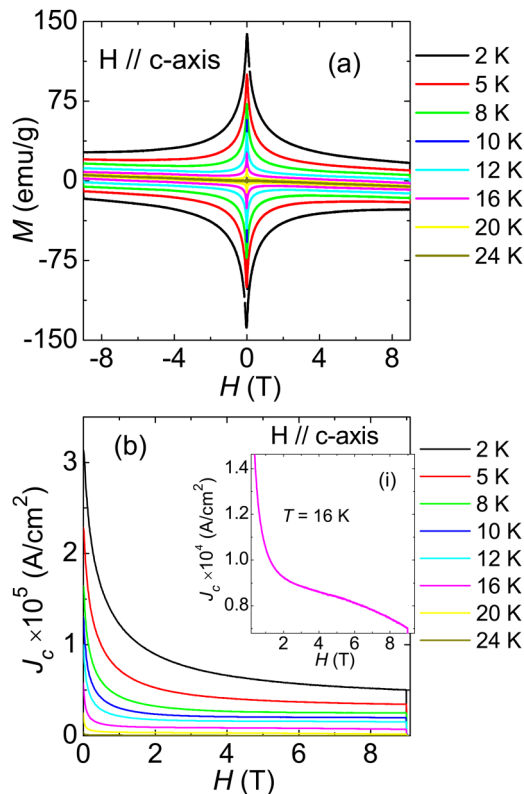

FIG. 2. (a) Isothermal $M(H)$ curves as measured. (b) Isothermal $J_c(H)$ curves as obtained from the Bean model. The inset shows details of $J_c(H)$ curve at 16 K, showing a change in curvature as $J_c(H)$ decays.
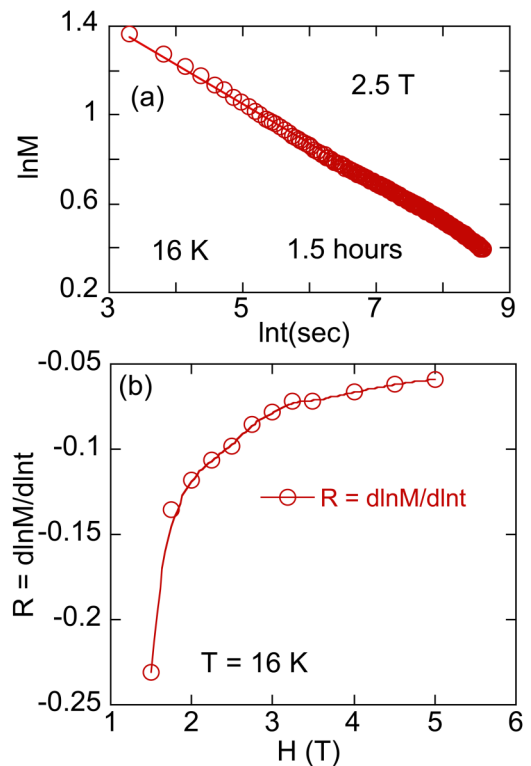

FIG. 3. (a) A typical magnetic relaxation curve measured during 1.5 h, showing usual linear time dependence. (b) Relaxation rate, $R = -d[\ln(M)]/d[\ln t]$, for $T = 1$ K, plotted as a function of the magnetic field.

Figure 4(a) shows a plot of U_0 vs. T for $H = 3\,\text{T}$. Two different slopes at intermediate temperature suggest a change in the pinning mechanism. Figure 4(b) shows a plot of the apparent activation pinning energy, $U_0 = R/T$, against $1/J_c$, obtained for $H = 3\,\text{T}$, which despite the fact that the values of the exponents do
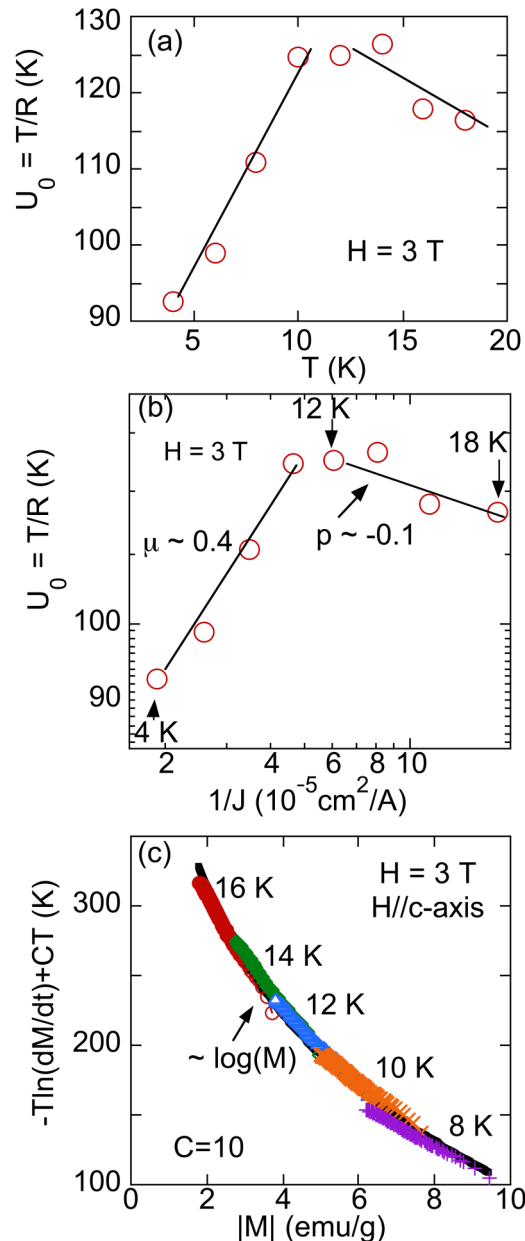
not correspond to the expected ones[31] ($\mu \sim 1$ and $p \sim -0.5$), the overall behavior suggests the existence of a crossover in the pinning mechanism of the type elastic to plastic occurring at some temperature between 10 K and 14 K.[31] This crossover has been associated with the fish-tail effect found in $M(H)$ curves,[31] which is absent in our curves. Similarly, in K-doped $BaFe_2As_2$, a pinning crossover is suggested through the U_0 vs. $1/J$ plot; however, no fish-tail effect is observed for that temperature range.[30] Therefore, it would be misleading to interpret the behaviour of R vs. T and U_0 vs. $1/J$ plots as a pinning crossover because there is no effect of such crossover in the measured isothermal $M(H)$ curves. Figure 4(c) shows a plot of the activation energy $U = -T\ln(dM/dt) + CT$ as obtained in Ref. 32, where the smooth curve was obtained with a constant $C = 10$. Parameter C depends on the attempt frequency, hoping distance, and sample dimension. It must be mentioned that the smooth curve following a $\log(M)$ behavior, as in Ref. 32 for YBaCuO, was obtained without the need of a temperature scaling. Also, the values of U in Fig. 4(c) are of the same order of magnitude of the values found for YBaCuO in Ref. 32 at similar reduced temperatures. The scaling of $U(M)$ with magnetic field for data obtained at $T = 16\,\text{K}$, as performed in Refs. 33–35, would point to a possible pinning crossover, as suggested in Fig. 3(b). Nevertheless, we could not find any reasonable scaling at this temperature.

Figure 5 shows the vortex phase-diagram where the values of H_{irr} are very close to values of $T_c(H)$. Such a wide irreversible region, as shown in Fig. 2(a), suggests that the studied system has potential for applications. In the phase-diagram (Fig. 5), at high temperatures, $T_c(H)$ increases linearly with $dH_{c2}(T)/dT = -3.1\,\text{T/K}$, which from the Werthamer-Helfand-Hohenberg (WHH) formula[36] renders $H_{c2}(0) = -0.695\,T_c$ and $dH_{c2}(T)/dT = 58\,\text{T}$. This value is higher than the Pauli paramagnetic limit for $H_{c2}(0)$ given by $H_p = 1.84$ and $T_c = 50\,\text{T}$.[37] The Maki parameter[36] defined as $\alpha = H_{c2}(0)/\sqrt{2}H_p = 0.82$ for the studied sample. Systems possessing

FIG. 4. (a) A plot of U_0 vs. T for $H = 3\,\text{T}$. (b) Apparent activation energy, U_0 obtained from the magnetic relaxation for $H = 3\,\text{T}$, plotted against $1/J_c(T)$. (c) Activation energy curve obtained from Maley's approach for $H = 3\,\text{T}$, plotted against magnetization.

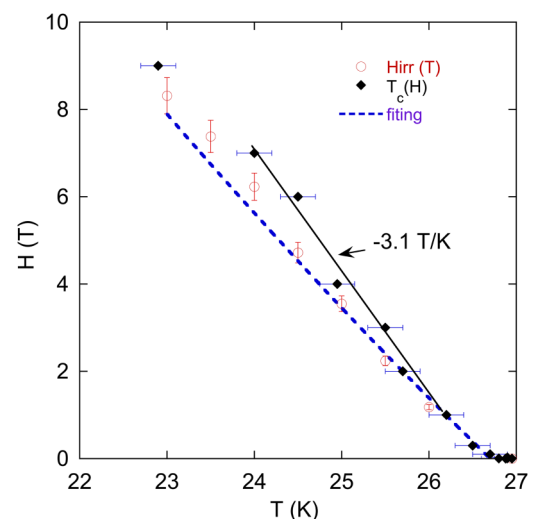**FIG. 5.** Vortex phase-diagram of $La_{0.34}Na_{0.66}Fe_2As_2$. The dotted line is a fitting to the irreversibility line curve (see text for details).

$\alpha > 1$ are candidates to exhibit the exotic Fulde-Ferrell-Larkin-Ovchinnikov (FFLO) phase.[38,39] Since our system has an anisotropy $\gamma = 1.9$,[11] the FFLO phase is a candidate to appear for $H \parallel ab$ planes. We observed that the irreversibility line does not follow a power law behavior with $(T_c - T)$ as is commonly observed in many superconductors. In addition, the proximity of the irreversibility line to the $T_c(H)$ line resembles the behavior observed in low T_c systems, as, for instance, in NbSe$_2$.[40] $H_{irr}(T)$ has been described in Refs. 41 and 42 by an expression which takes into account the disorder in the system. Even for NbSe$_2$, the $H_{irr}(T)$ line is visibly further apart from the $H_{c2}(T)$ line than what is observed in our sample. The dotted line in Fig. 5 represents the best fit of the $H_{irr}(T)$ data to the expression provided in Refs. 41 and 42, which is mentioned in the following:

$$1 - t - b + 3n_p(1 - t)^2 \, 4\pi - 2 \, \sqrt{2G_i} \, tb = 0,$$

where $t = T/T_c$ is the reduced temperature, $b = H/H_{c2}(0)$, n_p measures the disorder in the system, and G_i is a different definition of the Ginzburg number which measures the importance of thermal fluctuations. In that expression, b, n_p, and G_i are fitting parameters, and the dotted line shown in Fig. 5 was obtained for a slightly higher $T_c = 28$ K, $n_p = 0.002$, $G_i \sim 10^{-8}$, and $H_{c2}(0) = 60$ T. It is observed that both G_i and n_p show a good fit within 10% of the fitted values, whereas $H_{c2}(0)$ may vary within 4% of the value obtained from the fitting. The value of n_p is similar to that obtained in Ref. 41 for NbSe$_2$, $H_{c2}(0)$ is similar to the value obtained from the WHH expression, but G_i is three orders of magnitude lower than the value obtained for NbSe$_2$. We do not have explanation for such a low value of G_i in the present case. The importance of thermal fluctuations is sometimes associated with the extension of

the reversible region, which in our case is virtually absent from the $M(T)$ curves.

We present in Fig. 6(a), the plot of the normalized pinning force density, F_p/F_{pmax}, as a function of the reduced magnetic field $h = H/H_{irr}$, where $F_p = J_c \times H$. The collapse of the many different isothermal pinning force curves is evident on the graph. This plot allows us to obtain the reduced magnetic field (h) for which the pinning force reaches its maximum, $h_{max} = 0.45$, and a fitting of the resulting curve to the Dew-Hughes formula[23] $F_p/F_{pmax} = Ah^p(1 - h)^q$ produced $A = 5.14$, $p = 1.08$, and $q = 1.32$, where $p/(p + q) = h_{max} = 0.45$ as obtained from the experimental data. This fitting has been applied to examine the pinning force on many systems over the years,[43] and the different values obtained for the parameters h_{max}, p, and q are used to determine the type of the dominant pinning.[23,43–45] In a classic paper, Dew-Hughes discussed the various scenarios of pinning centers involved in different pinning mechanisms.[23] For a system having pinning due to the variation in the charge carrier mean free path (δl-pinning) and the pinning centers are point-like, the maximum in the normalized pinning force density occurs at $h = 0.33$, with $p = 1$ and $q = 2$. In the case of the pinning due to the variation in the superconducting transition temperature (δT_c-pinning), the maximum in the normalized pinning force density is found to be at much higher h values, in short, for point pinning centers, $h = 0.67$, with $p = 1$, $q = 2$; for surface pinning centers, $h = 0.6$, with $p = 1.5$ and $q = 1$; and for volume pinning centers, $h = 0.5$, with $p = q = 1$. Therefore, in the present study, $h = 0.45$ with $p = 1.08$ and $q = 1.32$ shows that a single type of pinning is not sufficient to explain the results. However, similar values of h have also been observed in many other studies of iron-pnictide superconductors, such as for BaFe$_{1.9}$Ni$_{0.1}$As$_2$, $h = 0.4$,[45] for Ca$_{0.8}$La$_{0.2}$Fe$_{1-x}$Co$_x$As$_2$, $h = 0.44$,[31] for Ba$_{0.68}$K$_{0.32}$Fe$_2$As$_2$, $h = 0.43$,[46] and for Ba(Fe$_{1-x}$Co$_x$)$_2$As$_2$, $h = 0.45$.[47] In such studies, the value of $h \approx 0.45$ is attributed to an inhomogeneous distribution of dopants or Arsenic deficiency.[46] Shahbazi et al.[45] argued that $h = 0.4$ in the case of BaFe$_{1.9}$Ni$_{0.1}$As$_2$ is due to the δl-type pinning. Zhou et al.[31] related $h = 0.44$ with the randomly distributed nanoscale point-like defects, which is common in the case of iron pnictide superconductors.[31,46,48] Therefore, $h = 0.45$ in our case is attributed to the δl-type pinning due to point pinning centers, whereas for δT_c pinning, the maximum in normalized pinning force density would occur at h higher than 0.5. The type of pinning can be further examined following an approach developed in Ref. 22, where the temperature dependent critical current at zero field $J_c(T)$, normalized by the critical current at zero field at $T = 0$, is plotted against $t = T/T_c$. The equivalent plot for our data is shown in Fig. 6(b), which is compared to the theoretical expression for δl-type of pinning, where $J_c(T)/J_c(0) = (1 + t^2)^{-1/2}(1 - t^2)^{5/2}$ and for δT_c-type pinning, $J_c(T)/J_c(0) = (1 - t^2)^{7/6}(1 + t^2)^{5/6}$.[22] It is evident from Fig. 6(b) that the δl-type pinning alone cannot explain the experimental data adequately.

IV. CONCLUSIONS

In conclusion, the vortex phase-diagram of the newly synthesized iron-based superconductor La$_{0.34}$Na$_{0.66}$Fe$_2$As$_2$ shows an irreversibility line very close to the mean field transition temperature $T_c(H)$ evidencing a strong pinning. The irreversibility line does not
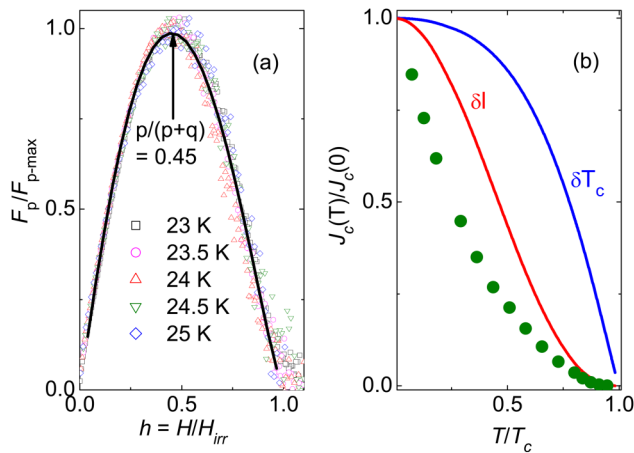

FIG. 6. (a) Normalized pinning force density plotted against the reduced magnetic field. The experimental data taken at different temperatures collapsed into a single scaled curve, which is fitted using the expression, $F_p/F_{pmax} = Ah^p(1 - h)^q$, where p and q are fitting parameters, which define the pinning characteristics. (b) Normalized critical current density, $J_c(T)/J_c(0)$, as a function of reduced temperature, T/T_c. The solid lines represent the δl and δT_c pinning behavior.

follow the usual power law with $(T_c - T)$, but it was successfully fitted by an expression developed in Refs. 41 and 42, considering the effect of disorder, where a considerably low disorder similar to that observed for NbSe$_2$[41,42] was found for our system. We observed that the upper critical field at zero temperature exceeds the prediction of the Pauli paramagnetic limit, suggesting that the system is a candidate to show the FFLO phase for $H \| ab$-planes. The critical current density at the zero magnetic field reaches the threshold value $J_c > 10^5 \, \text{A/cm}^2$ for temperatures below 12 K, which, along with the fact that the irreversibility line is very close to $T_c(H)$, makes the system technologically relevant. The magnetic relaxation obtained as a function of field for a fixed temperature shows that the relaxation rate monotonically decreases as the field increases, while the magnetic relaxation obtained for a fixed field as a function of temperature suggests a crossover in the pinning mechanism. The latter results allowed us to obtain a smooth curve of the isofield activation energy with magnetization, as first done by Maley,[32] where the observed $\log(M)$ behavior and values are similar to the ones obtained in Ref. 32 for YBaCuO. The pinning analysis using the Dew-Hughes model suggests a δl-type pinning due to the point pinning centers. However, the temperature dependence of the critical current density indicates that δl pinning alone cannot explain the data adequately. To explore this compound for technological use, the effect of grain boundaries on the critical current density and vortex dynamics in polycrystalline and thin film samples is yet to be investigated.

ACKNOWLEDGMENTS

REFERENCES

[1]F. Wang and D.-H. Lee, "The electron-pairing mechanism of iron-based superconductors," Science **332**, 200 (2011).
[2]P. Zhang, Z. Wang, X. Wu, K. Yaji, Y. Ishida, Y. Kohama, G. Dai, Y. Sun, C. Bareille, K. Kuroda *et al.*, "Multiple topological states in iron-based superconductors," Nat. Phys. **15**, 41–47 (2019).
[3]H. Hosono, A. Yamamoto, H. Hiramatsu, and Y. Ma, "Recent advances in iron-based superconductors toward applications," Mater. Today **21**, 278 (2018).
[4]I. Pallecchi, M. Eisterer, A. Malagoli, and M. Putti, "Application potential of Fe-based superconductors," Supercond. Sci. Technol. **28**, 114005 (2015).
[5]S. Aswartham, M. Abdel-Hafiez, D. Bombor, M. Kumar, A. U. B. Wolter, C. Hess, D. V. Evtushinsky, V. B. Zabolotnyy, A. A. Kordyuk, T. K. Kim, S. V. Borisenko, G. Behr, B. Büchner, and S. Wurmehl, "Hole doping in

BaFe$_2$As$_2$: The case of Ba$_{1-x}$Na$_x$Fe$_2$As$_2$ single crystals," Phys. Rev. B **85**, 224520 (2012).
[6]M. Abdel-Hafiez, P. J. Pereira, S. A. Kuzmichev, T. E. Kuzmicheva, V. M. Pudalov, L. Harnagea, A. A. Kordyuk, A. V. Silhanek, V. V. Moshchalkov, B. Shen, H.-H. Wen, A. N. Vasiliev, and X.-J. Chen, "Lower critical field and SNS-Andreev spectroscopy of 122-arsenides: Evidence of nodeless superconducting gap," Phys. Rev. B **90**, 054524 (2014).
[7]M. Abdel-Hafiez, Y. Zhang, Z. He, J. Zhao, C. Bergmann, C. Krellner, C.-G. Duan, X. Lu, H. Luo, P. Dai, and X.-J. Chen, "Nodeless superconductivity in the presence of spin-density wave in pnictide superconductors: The case of BaFe$_{2-x}$Ni$_x$As$_2$," Phys. Rev. B **91**, 024510 (2015).
[8]V. Grinenko, S.-L. Drechsler, M. Abdel-Hafiez, S. Aswartham, A. U. B. Wolter, S. Wurmehl, C. Hess, K. Nenkov, G. Fuchs, D. V. Efremov, B. Holzapfel, J. van den Brink, and B. Büchner, "Disordered magnetism in superconducting KFe$_2$As$_2$ single crystals," Phys. Status Solidi B **250**, 593 (2013).
[9]A. Iyo, K. Kawashima, S. Ishida, H. Fujihisa, Y. Gotoh, H. Eisaki, and Y. Yoshida, "Superconductivity on hole-doping side of (La$_{0.5-x}$Na$_{0.5+x}$)Fe$_2$As$_2$," J. Am. Chem. Soc. **140**, 369 (2018).
[10]J.-Q. Yan, S. Nandi, B. Saparov, P. Cermak, Y. Xiao, Y. Su, W. T. Jin, A. Schneidewind, and Th. Brückel, "Magnetic and structural transitions in La$_{0.4}$Na$_{0.6}$Fe$_2$As$_2$ single crystals," Phys. Rev. B **91**, 024501 (2015).
[11]Y. Gu, J.-O. Wang, X. Ma, H. Luo, Y. Shi, and S. Li, "Single-crystal growth of the iron-based superconductor La$_{0.34}$Na$_{0.66}$Fe$_2$As$_2$," Supercond. Sci. Technol. **31**, 125008 (2018).
[12]B. Rosenstein, B. Ya. Shapiro, I. Shapiro, Y. Bruckental, A. Shaulov, and Y. Yeshurun, "Peak effect and square-to-rhombic vortex lattice transition in La$_{2-x}$Sr$_x$CuO$_4$," Phys. Rev. B **72**, 144512 (2005).
[13]S. Salem-Sugui, Jr., L Ghivelder, A. D. Alvarenga, L. F. Cohen, H. Luo, and X. Lu, "Vortex dynamics as a function of field orientation in BaFe$_{1.9}$Ni$_{0.1}$As$_2$," Supercond. Sci. Technol. **26**, 025006 (2013).
[14]S. Salem-Sugui, Jr., J Mosqueira, A. D. Alvarenga, D. Sóñora, E. P. Herculano, D. Hu, G. Chen, and H. Luo, "Observation of an anomalous peak in isofield $M(T)$ curves in BaFe$_2$(As$_{0.68}$P$_{0.32}$)$_2$ suggesting a phase transition in the irreversible regime," Supercond. Sci. Technol. **28**, 055017 (2015).
[15]G Prando, R Giraud, S Aswartham, O Vakaliuk, M Abdel-Hafiez, C. Hess, S. Wurmehl, A. U. B Wolter, and B. Büchner, "Evidence for a vortex-glass transition in superconducting Ba(Fe$_{0.9}$Co$_{0.1}$)$_2$As$_2$," J. Phys. Condens. Matter **25**, 505701 (2013).
[16]S. Eley, M. Miura, B. Maiorov, and L. Civale, "Universal lower limit on vortex creep in superconductors," Nat. Mater. **16**, 409 (2017).
[17]H. Q. Yuan, J. Singleton, F. F. Balakirev, S. A. Baily, G. F. Chen, J. L. Luo, and N. L. Wang, "Nearly Isotropic superconductivity in (Ba, K)Fe$_2$As$_2$," Nature **457**, 565 (2009).
[18]J. D. Weiss, C. Tarantini, J. Jiang, F. Kametani, A. A. Polyanskii, D. C. Larbalestier, and E. E. Hellstrom, "High intergrain critical current density in fine-grain (Ba$_{0.6}$K$_{0.4}$)Fe$_2$As$_2$ wires and bulks," Nat. Mater. **11**, 682 (2012).
[19]C. Senatore, R. Flükiger, M. Cantoni, G. Wu, R. H. Liu, and X. H. Chen, "Upper critical fields well above 100 T for the superconductor SmFeAsO$_{0.85}$F$_{0.15}$ with $T_c = 46$ K," Phys. Rev. B **78**, 054514 (2008).
[20]R. Zhi-An, L. Wei, Y. Jie, Y. Wei, S. Xiao-Li, L. Zheng-Cai, C. Guang-Can, D. Xiao-Li, S. Li-Ling, Z. Fang, and Z. Zhong-Xian, "Superconductivity at 55 K in iron-based F-doped layered quaternary compound Sm[O$_{1-x}$F$_x$]FeAs," Chin. Phys. Lett. **25**, 2215 (2008).
[21]S. J. Singh, M. Bristow, W. R. Meier, P. Taylor, S. J. Blundell, P. C. Canfield, and A. I. Coldea, "Ultrahigh critical current densities, the vortex phase diagram, and the effect of granularity of the stoichiometric high-T_c superconductor CaKFe$_4$As$_4$," Phys. Rev. Mater. **2**, 074802 (2018).
[22]R. Griessen, W. Hai-hu, A. J. J. van Dalen, B. Dam, J. Rector, H. G. Schnack, S. Libbrecht, E. Osquiguil, and Y. Bruynseraede, "Evidence for mean free path fluctuation induced pinning in YBa$_2$Cu$_3$O$_7$ and YBa$_2$Cu$_4$O$_8$ films," Phys. Rev. Lett. **72**, 1910 (1994).
[23]D. Dew-Hughes, "Flux pinning mechanisms in type II superconductors," Philos. Mag. **30**, 293 (1974).

[24]C. P. Bean, "Magnetization of high-field superconductors," Rev. Mod. Phys. **36**, 31 (1964).

[25]A. Umezawa, G. W. Crabtree, J. Z. Liu, H. W. Weber, W. K. Kwok, L. H. Nunez, T. J. Moran, and C. H. Sowers, "Enhanced critical magnetization currents due to fast neutron irradiation in single-crystal $YBa_2Cu_3O_{7-\delta}$," Phys. Rev. B **36**, 7151 (1987).

[26]T. Ozak, L. Wu, C. Zhang, J. Jaroszynski, W. Si, J. Zhou, Y. Zhu, and Q. Li, "A route for a strong increase of critical current in nanostrained iron-based superconductors," Nat. Commun. **7**, 13036 (2016).

[27]D. Song, S. Ishida, A. Iyo, M. Nakajima, J.-i. Shimoyama, M. Eisterer, and H. Eisaki, "Distinct doping dependence of critical temperature and critical current density in $Ba_{1-x}K_xFe_2As_2$ superconductor," Sci. Rep. **6**, 26671 (2016).

[28]S. Ishida, D. Song, H. Ogino, A. Iyo, H. Eisaki, M. Nakajima, J.-i. Shimoyama, and M. Eisterer, "Doping-dependent critical current properties in K, Co, and P-doped $BaFe_2As_2$ single crystals," Phys. Rev. B **95**, 014517 (2017).

[29]S. Sundar, S. Salem-Sugui, Jr., E. Lovell, A. Vanstone, L. F. Cohen, D. Gong, R. Zhang, X. Lu, H. Luo, and L. Ghivelder, "Doping dependence of the second magnetization peak, critical current density, and pinning mechanism in $BaFe_{2-x}Ni_xAs_2$ pnictide superconductors," ACS Appl. Electron. Mater. **1**, 179–188 (2019).

[30]S. Sundar, S. Salem-Sugui, Jr., H. S. Amorim, H.-H. Wen, K. A. Yates, L. F. Cohen, and L. Ghivelder, "Plastic pinning replaces collective pinning as the second magnetization peak disappears in the pnictide superconductor $Ba_{0.75}K_{0.25}Fe_2As_2$," Phys. Rev. B **95**, 134509 (2017).

[31]W. Zhou, X. Xing, W. Wu, H. Zhao, and Z. Shi, "Second magnetization peak effect, vortex dynamics, and flux pinning in 112-type superconductor $Ca_{0.8}La_{0.2}Fe_{1-x}Co_xAs_2$," Sci. Rep. **6**, 22278 (2016).

[32]M. P. Maley, J. O. Willis, H. Lessure, and M. E. McHenry, "Dependence of flux-creep activation energy upon current density in grain-aligned $YBa_2Cu_3O_{7-x}$," Phys. Rev. B **42**, 2639 (1990).

[33]Y. Abulafia, A. Shaulov, Y. Wolfus, R. Prozorov, L. Burlachkov, Y. Yeshurun, D. Majer, E. Zeldov, H. Wuhl, V. B. Geshkenbein, and V. M. Vinokur, "Plastic vortex creep in $YBa_2Cu_3O_{7-x}$ crystals," Phys. Rev. Lett. **77**, 1596 (1996).

[34]S. Sundar, J. Mosqueira, A. D. Alvarenga, D. Sóñora, A. S. Sefat, and S. Salem-Sugui, Jr., "Study of the second magnetization peak and the pinning behaviour in $Ba(Fe_{0.935}Co_{0.065})_2As_2$ pnictide superconductor," Supercond. Sci. Technol. **30**, 125007 (2017).

[35]S. Salem-Sugui, Jr., L. Ghivelder, A. D. Alvarenga, L. F. Cohen, K. A. Yates, K. Morrison, J. L. Pimentel, Jr., H. Luo, Z. Wang, and H.-H. Wen, "Flux

dynamics associated with the second magnetization peak in the iron pnictide $Ba_{1-x}K_xFe_2As_2$," Phys. Rev. B **82**, 054513 (2010).

[36]N. R. Werthamer, E. Helfand, and P. C. Hohenberg, "Temperature and purity dependence of the superconducting critical field, H_{c2}. III. Electron spin and spin-orbit effects," Phys. Rev. **147**, 295 (1966).

[37]A. M. Clogston, "Upper limit for the critical field in hard superconductors," Phys. Rev. Lett. **9**, 266 (1962).

[38]P. Fulde and R. A. Ferrell, "Superconductivity in a strong spin-exchange field," Phys. Rev. **135**, A550 (1964).

[39]A. I. Larkin and Yu. N. Ovchinnikov, "Nonuniform state of superconductors," Sov. Phys. JETP **20**(3), 762–770 (1965).

[40]S. S. Banerjee, S. Saha, N. G. Patil, S. Ramakrishnan, A. K. Grover, S. Bhattacharya, G. Ravikumar, P. K. Mishra, T. V. C. Rao, V. C. Sahni, C. V. Tomy, G. Balakrishnan, D. Mck. Paul, and M. J. Higgins, "Generic phase diagram for vortex matter via a study of peak effect phenomenon in crystals of $2H-NbSe_2$," Physica C **308**, 25 (1998).

[41]B. Rosenstein and V. Zhuravlev, "Quantitative theory of transport in vortex matter of type-II superconductors in the presence of random pinning," Phys. Rev. B **76**, 014507 (2007).

[42]B. Rosenstein and D. Li, "Ginzburg-Landau theory of type II superconductors in magnetic field," Rev. Mod. Phys. **82**, 109 (2010).

[43]M. R. Koblischka and M. Muralidhar, "Pinning force scaling analysis of Fe-based high-T_c superconductors," Int. J. Mod. Phys. B **30**, 1630017 (2016).

[44]Md. Matin, L. S. Sharath Chandra, M. K. Chattopadhyay, R. K. Meena, R. Kaul, M. N. Singh, A. K. Sinha, and S. B. Roy, "Magnetic irreversibility and pinning force density in the Ti-V alloys," J. Appl. Phys. **113**, 163903 (2013).

[45]M. Shahbazi, X. L. Wang, K. Y. Choi, and S. X. Dou, "Flux pinning mechanism in $BaFe_{1.9}Ni_{0.1}As_2$ single crystals: Evidence for fluctuation in mean free path induced pinning," App. Phys. Lett. **103**, 032605 (2013).

[46]D. L. Sun, Y. Liu, and C. T. Lin, "Comparative study of upper critical field H_{c2} and second magnetization peak H_{sp} in hole- and electron-doped $BaFe_2As_2$ superconductor," Phys. Rev. B **80**, 144515 (2009).

[47]A. Yamamoto, J. Jaroszynski, C. Tarantini, L. Balicas, J. Jiang, A. Gurevich, D. C. Larbalestier, R. Jin, A. S. Sefat, M. A. McGuire, B. C. Sales, D. K. Christen, and D. Mandrus, "Small anisotropy, weak thermal fluctuations, and high field superconductivity in Co-doped iron pnictide $Ba(Fe_{1-x}Co_x)_2As_2$," Appl. Phys. Lett. **94**, 062511 (2009).

[48]H. Yang, H. Luo, Z. Wang, and H.-H. Wen, "Fishtail effect and the vortex phase diagram of single crystal $Ba_{0.6}K_{0.4}Fe_2As_2$," Appl. Phys. Lett. **93**, 142506 (2008).